100k Cycles and Beyond: Extraordinary Cycle Stability for MnO_2 Nanowires Imparted by a Gel Electrolyte Supporting Information

Mya Le Thai,[†] Girija Thesma Chandran,[†] Rajen K. Dutta,[‡] Xiaowei Li,[¶] and Reginald M. Penner[*,†]

†*Department of Chemistry, University of California, Irvine, CA 92697*

‡*Department of Physics and Astronomy, University of California, Irvine, CA 92697*

¶*Department of Chemical Engineering and Materials Science, University of California, Irvine, CA 92697*

Au@δ-MnO_2 Nanowire Fabrication. Here we provide a detailed process flow (Figure S1) and description of the procedure for fabricating Au@δ-MnO_2 Core@Shell Nanowire Capacitors. Starting with 2" $\times$ 0.5" glass squares, a 40 nm layer of nickel is thermally evaporated. A positive photoresist layer (PR, Shipley, S1808) is then deposited on the nickel film by spin-coating and soft-baked (90°C for 30 min). The PR layer is then photo patterned using a chromium/quartz contact mask in conjunction with 365 nm UV light source equipped with a shutter and alignment stage (Newport, 83210i-line, 2.3 s). After exposure, the nascent pattern was developed for 20 s in developer solution (Shipley, MF-319). Then the nickel was removed from this patterned surface by etching with 0.8 M HNO_3 for 5 minutes (step 1). This step removed exposed nickel and also created an undercut at the edge of the PR. This undercut forms a horizontal trench which can be used to template the growth by electrodeposition of gold nanowires. Electrodeposition is accomplished by immersing the lithographically patterned region into a gold plating solution (Clean Earth Solutions^{TM}).

Gold nanowires are then deposited within this trench by potentiostatic growth at a potential of - 0.9 V versus SCE (saturated calomel reference electrode) for 1000 s (step 2). After electrodeposition is complete, the PR layer was removed using acetone (step 3). Photolithography is also used to prepared gold electrical contacts as shown in steps 4,5. Photoresist is then applied as in insulator atop the gold current collectors. These insulator layers are hard baked at 190 °C oven for a 30 minutes, rending the photoresist layer impervious to organic solvent.

In step 6, electrical contact is made to the gold contacts, and δ-MnO_2 is electrodeposited on the exposed gold nanowires from an aqueous plating solution containing 2 mM $Mn(ClO_4)_2$, 50mM $LiClO_4$. MnO_2 electrodeposition was carried out potentiostatically at +0.6 V versus MSE (saturated mercurous sulfate reference electrode) for a duration of 5 s–40 s, yielding shell thickness in the range from 143 - 300 nm. After deposition, the device was rinsed with water, air-dried, and baked at 90 °C for 30 minutes. Finally, 100 μL of 1M $LiClO_4$, 20 (w/w)% PMMA, PC gel electrolyte was drop-cast on the new complete device (step 7). At

room temperature, the gel electrolyte is too viscous to be transfered and casted. Therefore, prior to drop casting, the gel was heated to 115°C on a hot plate for 10 minutes until the stir bar was able to rotate. The small amount of gel as mentioned above was coated on to device using doctor blading method to form an evenly spread and fully covered layer of gel on the window where all the wires located. The complete device with gel electrolyte was put in vacuum desiccator to remove all air bubbles before measurement.

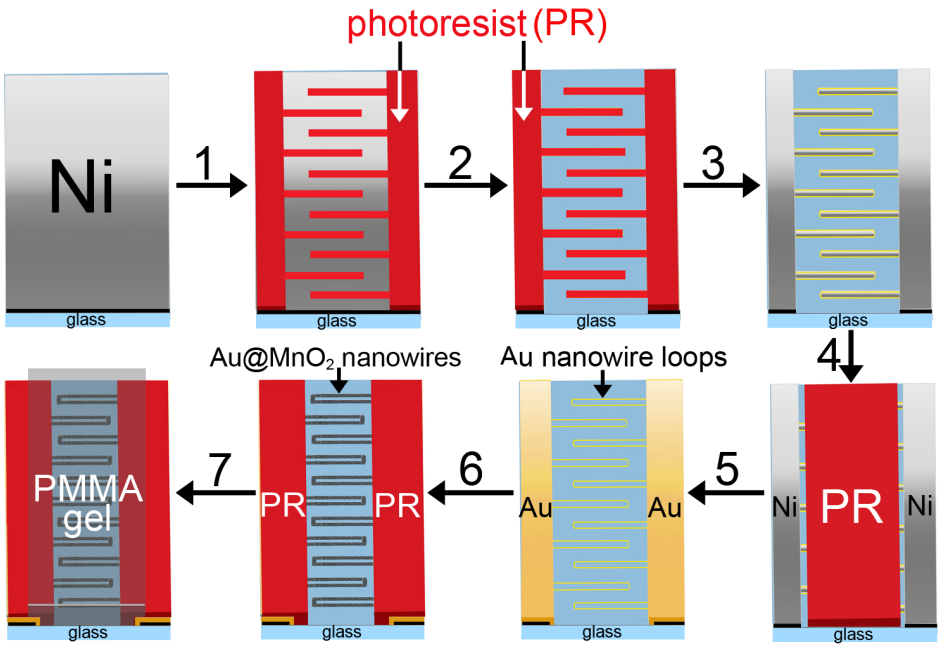

Figure S 1: Process flow for the fabrication by LPNE of Au@δ-MnO_2 core@shell nanowire array with gold contacts and PMMA gel electrolyte. Step 1: A nickel-coated glass slide is covered with photoresist and lithographically patterned using a contact mask, Step 2: Nickel is removed from exposed areas using nitric acid etching, producing a horizontal template, Step 3: Gold is electroplated into this template which coincides with the perimeter of the exposed region, Step 4: Gold nanowires, still anchored to nickel electrodes, are masked with photoresist, Step 5: Gold electrical contacts are evaporated, the photoresist layer is removed with acetone, and nickel is stripped using nitric acid, Step 6: Gold contacts are insulated with photoresist, and δ-MnO_2 is electrodeposited as a shell onto the gold nanowires, Step 7: PMMA gel electrolyte layer is drop-coated.

Deconvolution of Specific Capacitance. The total C_{sp} for Au@MnO_2 core@shell nanowire capacitor can be resolved into contributions from insertion capacitance and non-insertion capacitance by measuring the scan rate, ν, dependance of C_{sp} as a function of potential. Eq. (1) assumes that the component of the capacitive current associated with insertion will ex-

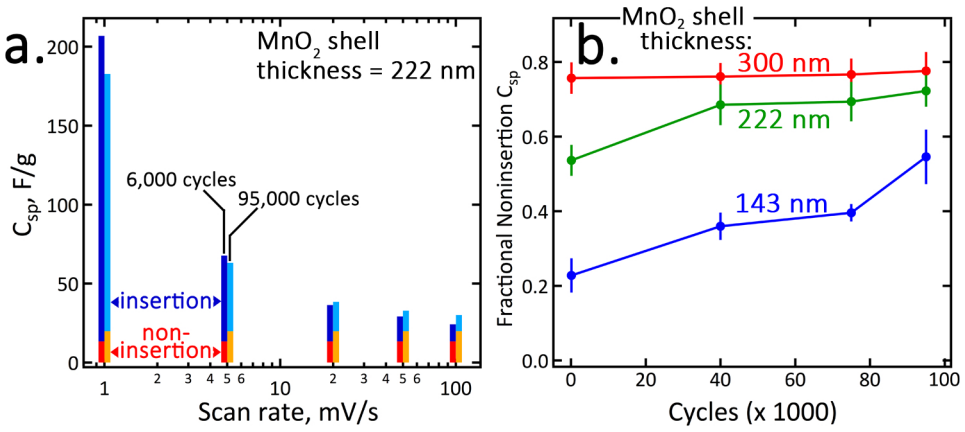

Figure S 2: Deconvolution of two contributions to C_{sp}: Faradaic insertion capacity ($\propto \nu^{1/2}$, blue and cyan) and noninsertion capacity ($\propto \nu$, red and yellow). a) Bar graphs of the two C_{sp} components versus ν. Results for 6,000th and 95,000th cycles are shown. Data shown for 222 nm MnO_2 shell thickness. b) Fraction of C_{sp} derived from noninsertion capacity as a function of number of charge/discharge cycles.

hibit diffusion control and scale linearly with $\nu^{1/2}$ while the noninsertion current will behave capactiviely (or pseudocapacitively) and scale linearly with ν:[1–4]

$$i_{E,total} = i_{E,noninsertion} + i_{E,insertion} = k_1\nu + k_2\nu^{1/2} \quad (1)$$

where k_1 and k_2 are scan rate independent constants. A plot of the insertion and noninsertion capacities versus scan rate for Au@MnO_2 nanowire capacitors cycled in liquid PC (6000 cycles) and PMMA gel (95,000 cycles) are nearly identical (Figure S2a). The fraction of the capacitance attributable to noninsertion increases as a function of cycling but a significant insertion component of 20 - 45% remains even after 95,000 cycles.(Figure S2b) The conclusion is that in the PMMA gel electrolyte, δ-MnO_2 shell retains significant Li^+ insertion/deinsertion capacity for more than 100,000 cycles.

Raman Microprobe Analysis. Representative Raman microprobe spectra for single nanowires are shown in Figure S3a. Spectra for s-prepared Au@δ-MnO_2 core@shell nanowires (red trace) show two peaks at 652 cm^{-1} and 572 cm^{-1} that are assigned to the symmetric

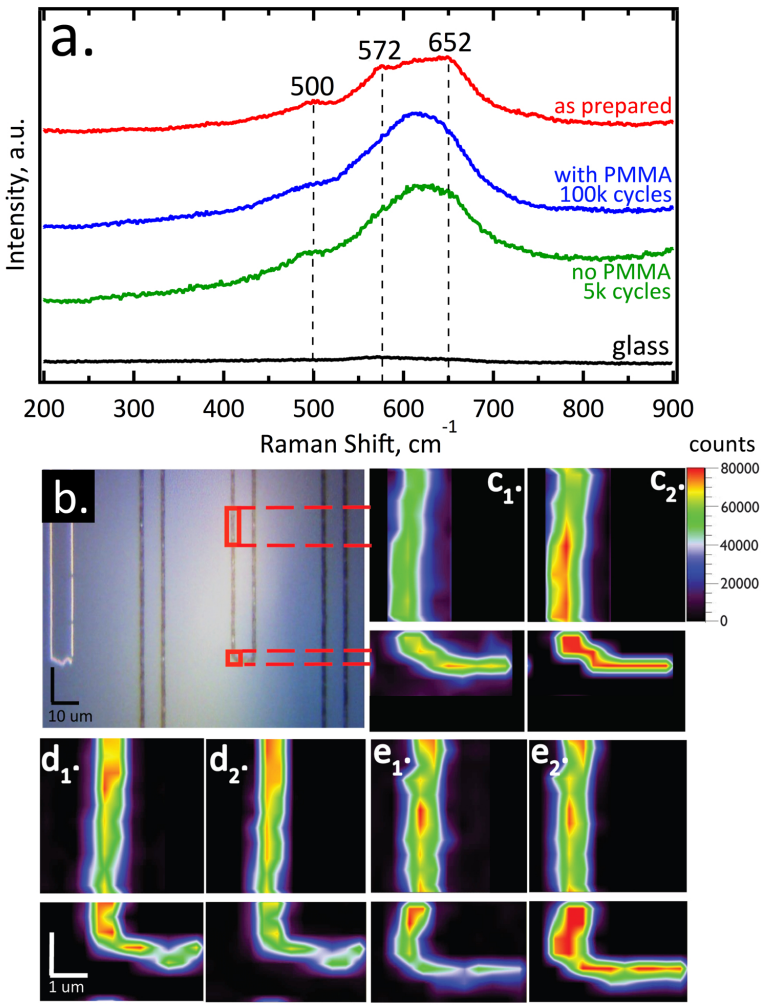

Figure S 3: (a) Raman spectra of Au@δ-MnO_2 core@shell nanowire at different state: as prepared condition (red trace), cycled in 1.0 M $LiClO_4$, PC electrolyte (green trace) and 1.0 M $LiClO_4$, PMMA: PC gel electrolyte (blue trace). (b) Optical micrograph of the interdigitated Au@δ-MnO_2 core@shell nanowires. (c,d,e) Color maps of integrated band intensities of the peaks 572 cm^{-1} (1) and 652 cm^{-1}(2) of (c) as prepared Au@δ-MnO_2 core@shell nanowire, (d) cycled in 1.0 M $LiClO_4$, PC electrolyte after 5,000 cycles and (e) 1.0 M $LiClO_4$, PMMA: PC gel electrolyte after 100,000 cycles.

stretching vibration (Mn–O) of the MnO_6 groups, and the (Mn–O) stretching aligned with the plane of the layers of MnO_6 sheets, respectively, in birnessite phase MnO_2.[5–9] A weaker transition at 500 cm^{-1}, observed prior work involving birnessite MnO_2, has not been definitively assigned.

Raman spectra obtained after the cycling of these nanowires in either PC and PC:PMMA gel electrolyte (Figure S3a, blue and green traces), are identical, and show a characteristic broadening of the 652 cm^{-1} and 572 cm^{-1} bands, that culminates in the merging of these bands to form a single broader peak at 625 cm^{-1}. This transformation, which has been previously observed,[5,6] is been attributed to the local lattice distortion of the MnO_2 structure caused by the insertion/deinsertion of cations. These spectra show no new bands, suggesting that no new phases/species are generated during the cycling process.

Raman mapping was also performed to look, more carefully, for local differences between nanowires cycled in PC and the PMMA gel electrolytes. An optical image of the region investigated (Figure S3b) encompasses both straight and linear nanowire regions. Raman maps c, d, and e, correspond to as prepared nanowires, nanowires cycled in 1M $LiClO_4$, PC for 5,000 cycles, and nanowires cycled in 1M $LiClO_4$, PC: PMMA gel electrolyte for 100,000 cycles, respectively. For each sample a-c, two maps are shown: map 1 (e.g., c_1, d_1, etc.) was acquired at 572 cm^{-1} and map 2 at 652 cm^{-1}. Although small differences can be identified between the three samples studied, for peaks at both energies, we see no significant differences in these maps between nanowires cycled in PC and the PMMA gel electrolytes. A more thorough Raman spectroscopy study will be required to reveal the subtle chemical and structural changes that are no doubt occurring in samples cycled in PC and PMMA gel electrolytes.

References

(1) Conway, B. *Electrochemical Supercapacitors: Scientific Fundamentals and Technological Applications (POD)*; Kluwer Academic/Plenum: New York, 1999.

(2) Liu, T.-C.; Pell, W.; Conway, B.; Roberson, S. Behavior of Molybdenum Nitrides as Materials for Electrochemical Capacitors Comparison with Ruthenium Oxide. *J. Electrochem. Soc.* **1998**, *145*, 1882–1888.

(3) Brezesinski, K.; Wang, J.; Haetge, J.; Reitz, C.; Steinmueller, S. O.; Tolbert, S. H.; Smarsly, B. M.; Dunn, B.; Brezesinski, T. Pseudocapacitive Contributions to Charge Storage in Highly Ordered Mesoporous Group V Transition Metal Oxides with Iso-oriented Layered Nanocrystalline Domains. *J. Am. Chem. Soc.* **2010**, *132*, 6982–6990.

(4) Wang, J.; Polleux, J.; Lim, J.; Dunn, B. Pseudocapacitive Contributions to Electrochemical Energy Storage in TiO_2 (anatase) Nanoparticles. *J. Phys. Chem. C* **2007**, *111*, 14925–14931.

(5) Chen, D.; Ding, D.; Li, X.; Waller, G. H.; Xiong, X.; El-Sayed, M. A.; Liu, M. Probing the Charge Storage Mechanism of a Pseudocapacitive MnO_2 Electrode Using in Operando Raman Spectroscopy. *Chem. Mater.* **2015**, *27*, 6608–6619.

(6) Hsu, Y.-K.; Chen, Y.-C.; Lin, Y.-G.; Chen, L.-C.; Chen, K.-H. Reversible Phase Transformation of MnO_2 Nanosheets in an Electrochemical Capacitor Investigated by In Situ Raman Spectroscopy. *Chem. Commun.* **2011**, *47*, 1252–1254.

(7) Julien, C.; Massot, M.; Baddour-Hadjean, R.; Franger, S.; Bach, S.; Pereira-Ramos, J. Raman Spectra of Birnessite Manganese Dioxides. *Solid State Ionics* **2003**, *159*, 345–356.

(8) Baddour-Hadjean, R.; Pereira-Ramos, J.-P. Raman Microspectrometry Applied to the Study of Electrode Materials for Lithium Batteries. *Chem. Rev.* **2009**, *110*, 1278–1319.

(9) Duay, J.; Sherrill, S. A.; Gui, Z.; Gillette, E.; Lee, S. B. Self-Limiting Electrodeposition of Hierarchical MnO_2 and $M(OH)_2/MnO_2$ Nanofibril/Nanowires: Mechanism and Supercapacitor Properties. *ACS Nano* **2013**, *7*, 1200–1214.